

1 **The crop residue conundrum: maintaining long-term soil organic carbon stocks**
2 **while reinforcing the bioeconomy, compatible endeavors?**

3 Christhel Andrade^{1,2,*}, Hugues Clivot³, Ariane Albers¹, Ezequiel Zamora-Ledezma⁴,
4 Lorie Hamelin¹

5 ¹ Toulouse Biotechnology Institute (TBI), INSA, INRAE UMR792, and CNRS
6 UMR5504, Federal University of Toulouse, 135 Avenue de Ranguel, F-31077,
7 Toulouse, France.

8 ² Department of Chemical, Biotechnological and Food Processes, Faculty of
9 Mathematical, Physics and Chemistry Sciences. Universidad Técnica de Manabí
10 (UTM), 130150 Portoviejo, Ecuador.

11 ³ Université de Reims Champagne Ardenne, INRAE, FARE, UMR A 614, 51097
12 Reims, France.

13 ⁴ Faculty of Agriculture Engineering. Universidad Técnica de Manabí (UTM), 13132
14 Lodana, Ecuador.

15 *Corresponding author: andraded@insa-toulouse.fr . ORCID: 0000-0002-2448-6186

16

17 **Supplementary Information 1 (SI1)**

18 **INDEX**

- 19 1. Pedoclimatic Data
20 2. Crop sequences
21 3. Bioeconomy technologies
22 4. AMGv2 adaption for bioeconomy

23 5. Sensitivity Analyses

24 Table S1.1. Crop residues considered to be exported for bioeconomy and the
25 technical harvestable fraction of the residues.

26 Table S1.2. Different combinations of parameters considered for sensitivity. The Cr
27 has been split between h_a and h_s

28 Fig S1. France Climate typologies

29 Fig S2. Dominant soil texture of the agricultural lands of France

30 Fig S3. Contribution of each type of crop to the total biomass production (grain
31 DM) in France (2020 – 2120 timeframe).

32 Fig SI 4. Sensitivity analyses (SA) for the pyrolysis scenario determined without the
33 active pool.

34 Fig SI 5. Sensitivity analyses (SA) for the pyrolysis scenario determined with the
35 active and stable pools.

36 Fig SI 6. Sensitivity analyses (SA) for the gasification scenario.

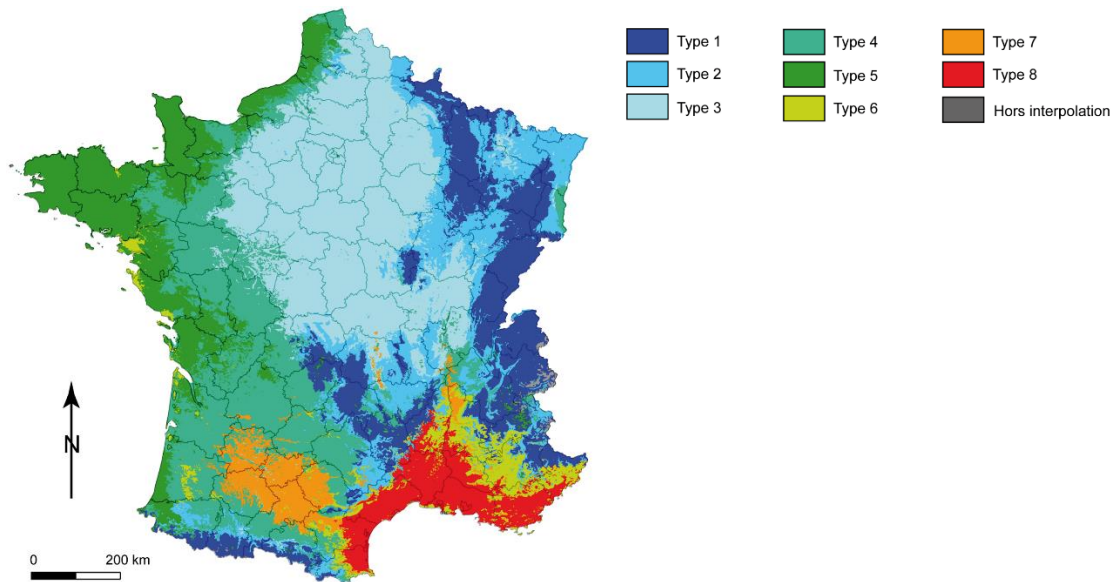
37 Fig SI 7. Sensitivity analyses (SA) for the hydrothermal liquefaction scenario.

38 Fig SI 8. Sensitivity analyses (SA) for the anaerobic digestion scenario.

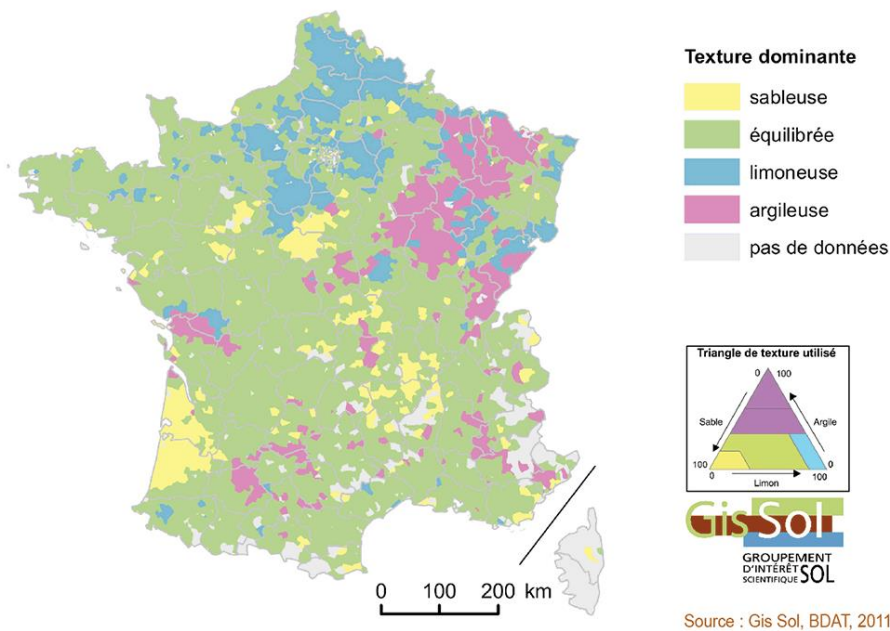
39 Fig SI 9. Sensitivity analyses (SA) for the lignocellulosic ethanol scenario.

40 **1. Pedoclimatic data**

41 The climate of France can be grouped into 8 typologies (Joly et al., 2010) as shown in
42 Fig S1, while the soil texture of the agricultural lands can be defined as sandy, balanced,
43 silty, or clayey (GisSol, 2011) according to Fig S2.



44 Fig S1. France climate typologies. Type 1: mountain climates, Type 2: the semi-
45 continental climate and the climate of the mountain margins, Type 3: The degraded
46 oceanic climate of the central and northern plains, Type 4: Altered oceanic climate,
47 Type 5: The frank oceanic climate, Type 6: The altered Mediterranean climate, Type 7:
48 The climate of the South-West Basin, Type 8: The frank Mediterranean climate, Hors
49 interpolation: Out of interpolation. (Joly et al., 2010).



50

51 Fig S2. Dominant soil textures of the agricultural lands of France. Sableuse : sandy,
 52 équilibrée : balanced, limoneuse : silty, argileuse : clayey, pas de données : no data.
 53 Retrieved from (GisSol, 2011).

54 The APCUs in Launay et al. (2021) were created using the SAFRAN grid while the
 55 climate data input to the model in this work came from DRIAS RCP4.5, therefore some
 56 points of the grid were lost during the adaptation. Besides, we used Launay et al. (2021)
 57 yields obtained from STICS modeling, where some simulation units were lost during
 58 the modeling, thus no yields were available for those units. Changing the climate grid
 59 and recycling the simulated yields are major differences from Launay et al. (2021) and
 60 resulted in 11784 APCU and 60390 simulation units in the present work vs 12060
 61 APCU and 62694 simulation units in Launay et al. (2021). This also affected the total
 62 area included in the study, **which decrease from 18.35 Mha to 14.89 Mha at the APCU**
 63 **level, and from 4.79 Mha to 3.48 Mha at the simulation units level.**

64 **2. Crop rotations**

65 The crop rotations were retrieved from Launay et al., (2021). Due to the high resolution
66 of the data, a total of 1472 crop rotations were included (or 1588 if we considered the
67 type of tillage as a differentiation in the rotation). The crops included in the rotations are
68 grain and silage maize, winter wheat, winter and spring peas, rapeseed, sunflower, and
69 sugar beet. The crop rotations also included temporary grasslands, alfalfa, and cover
70 crops (mustard and ray-grass). Temporary grasslands, alfalfa, and cover crops were not
71 considered to be exported for bioeconomy because they are already being fully used for
72 other purposes as animal bed and fodder (temporary grasslands and alfalfa) or are
73 generally left on soils to maintain N levels (cover crops).

74 The original retrieved data included only 33 years of information, with rotation
75 durations varying from 1 to 13 years. For the 100 years of modeling, we recycled the 33
76 years of original data. As a limitation of this work, the recycling of each 33 years meant
77 that for some simulation units the rotations at year 33 were not completed but the
78 following year 34 presented the crop corresponding to the first crop in the sequence.

79 The product yield of each crop depends on the pedoclimatic characteristics and farming
80 management; therefore, it varies among simulation units. We obtained the spatially
81 explicit yields from the STICS results modeled in Launay et al. (2021) and used the
82 average value for the 30 years considered there. This means that for a given simulation
83 unit, the grain yield in tonnes per ha of a given crop in the sequence will be the same
84 throughout the 100 years of the modeling done in this work.

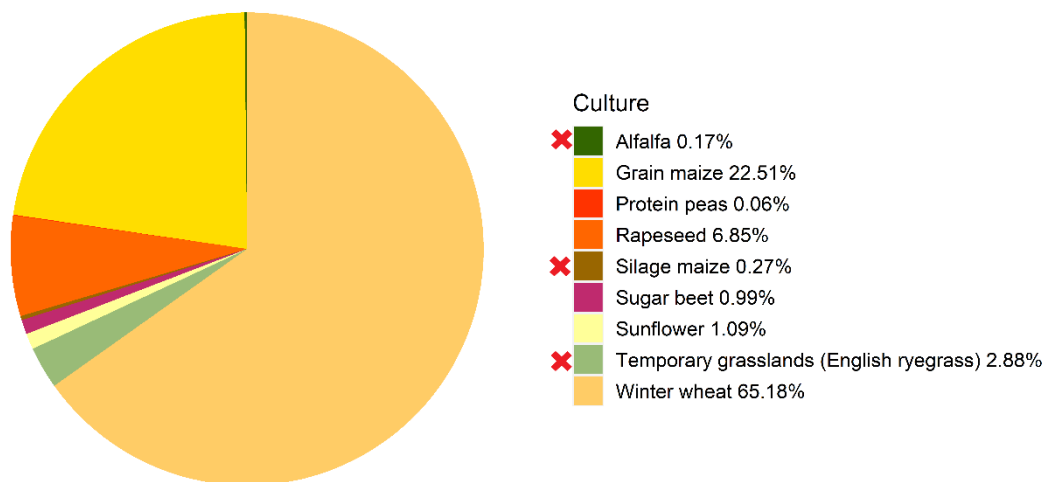
85 The total annual production of each crop (cover crops excluded) for the starting year
86 2020, as well as the technical harvestable fraction, are shown in Table S1.1. To
87 determine the most representative crop in arable lands in France we determined the
88 mean contribution of each crop for the whole mix of the considered crops for the 100
89 years' timeframe (Fig S3). The amount of crop residues currently exported is specific

90 for each simulation unit and varies among the years according to the crop sequences.
 91 However, on average for the 100 years at a national scale 466,656 tonnes grain ha⁻¹ y⁻¹
 92 (DM) are produced in the cropland surface included in this study, of which 46% of the
 93 residues are already being used for animals. The dataset containing the crop sequences,
 94 annual yields, and information about the current exporting of the crop sequences per
 95 simulation unit and the scripts to determine the total annual yield per crop, annual crop
 96 contribution to the mix, and annual percentage of crops exported are available in
 97 <https://doi.org/10.48531/JBRU.CALMIP/AUEEEJ>. It must be noted that crops
 98 indicating current exports refer to a 100% exporting rate of the harvestable crop residue.
 99 Table S1.1. Crop residues considered to be exported for bioeconomy and the technical
 100 harvestable fraction of the residues.

Crops included in this study	Crop residue considered for bioeconomy	Estimated biomass potential for crop residue at national scale (Mtonnes y⁻¹ DM)^a	Technical harvestable fraction of residues
Winter wheat ^b	YES	35.43	0.60
Grain maize	YES	14.15	0.70
Silage maize	NO	0.26	0
Protein peas ^c	YES	0.00	0.60
Rapeseed	YES	3.18	0.55
Sunflower	YES	0.89	0.80
Sugarbeet	YES	1.20	0.91
Alfalfa	NO	0.05	0

Temporary			
grasslands (English	NO	1.13	0
ryegrass)			
Potential biomass available for the		30.39	
bioeconomy ^c			

101 ^a Average yield for all the simulations units in the year 2021. The yields vary with the
102 year due to the crop rotations; ^b The crop rotations used here were the same as in
103 Launay et al. (2021). They performed the SOC simulations using STICS and all the
104 cereal-like crops (wheat, barley, oats, rice, etc.) were considered to be winter wheat.
105 Since we recycled the crop rotations, we also consider the ensemble of cereal-like crops
106 to be winter wheat; ^c winter peas and spring peas are considered as protein peas in
107 AMG, thus the total yield was calculated as a mixture of the two types of peas.
108 ^cTotal crop residues considered for bioeconomy minus the fraction already exported for
109 other services (46%).



110 Biomass amount contribution per crop (average for 100 years)

111 Fig. S3. Contribution of each type of crop to the total residual biomass production (DM)
112 in France (average for a 2020 – 2120 timeframe). Red cross (x) indicates crops not
113 harvested in the bioeconomy scenarios.

114 **3. Bioeconomy technologies**

115 The conditions assumed for each considered technology are briefly explained in this
116 section.

117 Pyrolysis: Pyrochar coproduct

118 Pyrolysis is a thermochemical process that converts the biomass to bio-oil at high
119 temperatures in the absence of oxidants, with the coproduction of gas and biochar,
120 henceforth referred to as pyrochar. The process can be classified as fast or slow
121 pyrolysis. Fast pyrolysis comprises mid-range temperatures and low times (300-500°C,
122 seconds to a few minutes), which enhance the production of bio-oil (75-50% bio-oil, 12-
123 20% pyrochar, 20-40% gas) (Malyan et al., 2021). Slow pyrolysis is carried out at high
124 temperatures and longer retention times (500-700°C, minutes), favoring higher yields of
125 pyrochar (30% bio-oil, 35% pyrochar) (Lehmann and Joseph, 2010). From an economic
126 point of view (i.e., higher yield of bio-oil), we consider the use of the crop residues in a
127 fast pyrolysis process.

128 Gasification: Gaschar coproduct

129 Gasification is a thermochemical process, which as opposed to pyrolysis, is carried out
130 in presence of an oxidant agent. Gasification generates syngas and co-products, such as
131 gaschar, tar, and ashes. Since gasification is carried out at higher temperatures than
132 pyrolysis (700-1200°C), it has been noted that a lower amount of biochar is produced
133 (10%) but of higher stability than that produced under pyrolysis processes (Molino et
134 al., 2016). In this study, we considered a gasification process carried out at temperatures

135 ranging from 800-1200°C, followed by the return of the resulting gaschar to the arable
136 lands. We did not consider the tar (undesirable co-product) nor the ashes (high in silica
137 and low in C) as EOM to the soil.

138 Hydrothermal Liquefaction: Hydrochar coproduct

139 Hydrothermal liquefaction (HTL) is a thermochemical process carried out at low
140 temperatures of around 280-370°C with retention times of around 20-30 minutes. HTL
141 uses wet biomass (15-20% dry matter) in contrast to pyrolysis and gasification, which
142 require a pre-treatment to dry the matter to >90% (Jahirul et al., 2012). HTL produces
143 bio-oil and a solid residue called “hydrochar”. Note that there is a similar process called
144 hydrothermal carbonization (HTC), in which the main product is hydrochar and not bio-
145 oil. HTC processes involve higher temperatures (300-450°C) over a longer period
146 comprising hours, making HTL hydrochar is constitutively different from HTC
147 hydrochar. Catalysts can enhance the efficiency of HTL processes, especially alkali
148 catalysts as K₂CO₃ (Seehar et al., 2021). We consider an HTL process at temperatures
149 ranges of 300-400°C aided by catalysts with the hydrochar as EOM to soils.

150 Anaerobic Digestion: Digestate coproduct

151 In the anaerobic digestion (AD) process the organic constituents of the biomass are
152 decomposed by microorganisms in the absence of oxygen. AD generates biogas, which
153 is composed of methane, carbon dioxide, and traces of other gases, as well as a by-
154 product known as digestate. AD uses a wide variety of biomass-based feedstock, which
155 could be wet (15-35% DM) or dry (10%). The most common AD processes co-digest
156 more than one substrate, at mesophilic temperatures (30-40°C) with retention times
157 varying according to the feedstock (typically 10-25 days). The AD scenario of this

158 study consists of a CR and manure (cattle, pig, and poultry) mixture, whereby the C
159 return to the soil is computed from CR only.

160 Lignocellulosic ethanol: Molasses coproduct

161 Bioethanol is a biofuel produced from the fermentation of sugars in the biomass and its
162 conversion into alcohol employing microorganisms (Swain et al., 2019). In this work,
163 we consider that CR are exposed to an acid pretreatment that frees cellulose and
164 hemicellulose, followed by the hydrolysis to glucose and xylose, which are fermented to
165 ethanol by the action of *Saccharomyces cerevisiae*, and finally purified by distillation
166 (Bušić et al., 2018). The unconverted fractions are directed to a residual stream known
167 as stillage, which is centrifuged to separate the liquid fraction (molasses) and the solid
168 fraction (Tonini et al., 2016). The solid fraction is normally used as an animal feed
169 supplement and for energy production in power plants, therefore, here we only consider
170 the return of the bioethanol molasses to the soils.

171 4. Carbon inputs from bioeconomy and AMGv2 adaption

172 Modifications were performed on AMGv2 to consider the input of the bioeconomy co-
173 products as C sources in the soil.

174 *2.1 Calculation of C inputs: Carbon conversion (Cc)*

175 We define C conversion (Cc) as the percentage of initial C in the biomass that is present
176 in the co-product. It is the mass of C in the solid co-product divided by the mass of C in
177 the initial dry biomass (Eq S1).

$$178 \quad \%Cc = \frac{BpY * BpC}{BmC} * 100 \quad (\text{Eq S1})$$

179 where Cc is the carbon conversion (%), BpY is the coproduct yield (kg Bp kg⁻¹
180 biomass), which corresponds to the amount of coproduct resulting from the treatment of

181 1 kg of feedstock during the bioeconomy process, BpC is the carbon content in the co-
182 product (kg C kg⁻¹ Bp), and BmC is the initial carbon content in the biomass (kg C kg⁻¹
183 biomass).

184 Andrade et al. (2022), reviewed the literature to determine the C pathway from crop
185 residues to understand the amount of feedstock C that is present in each coproduct
186 considered in this work. The study employed Eq S1 to determine the Cc coefficient used
187 for each technology. BmC was determined for each technology dataset ranging from
188 0.41-0.5 kg C kg⁻¹ biomass DM in Andrade et al. (2022).

189 Cc is a parameter fed to AMG that allows determining the C input based on the crop
190 yields. Cc was used in Eq (S2) to determine the amount of C from a given co-product
191 that would be applied in a given simulation unit per year.

$$192 \quad TBpC = Wt(dm)_i * WtCc_i * Cc \quad (\text{Eq S2})$$

193 where TBpC is the total coproduct C applied [t C ha⁻¹ y⁻¹], Wt(dm)_i is the crop residues
194 mass available for crop i [t crop residues ha⁻¹ y⁻¹], WtCc_i is the Crop residue carbon
195 content for crop residue i [t C t⁻¹ crop]. The suffix i denotes the different crops that
196 could be included in the rotation. AMG follows an annual timestep, therefore, it allows
197 to input only one main crop per year.

198 Wt(dm)_i is determined for each crop in each simulation unit based on the HI and
199 allocation coefficients (Bolinder et al., 2007) and the grain yield [t biomass DM ha⁻¹ y⁻¹]
200 input, while WtCC_i was defined as 0.444 g C g⁻¹ biomass DM (Clivot et al., 2019).

201 ***2.2 AMG adaptation: Carbon Recalcitrance (Cr) of bioeconomy coproducts***

202 The soil carbon partitioning in AMG is described by Eq S3 and Eq S4 (Clivot et al., 2019).

$$203 \quad QC = QC_S + QC_A \quad (\text{Eq S3})$$

204
$$\frac{dQC_A}{dt} = \sum_i m_i h_i - kQC_A \quad (\text{Eq S4})$$

205 where QC is the total SOC stock (t ha^{-1}), QC_A and QC_S are the C stocks of the active and
 206 stable C pools (t ha^{-1}) respectively, m_i is the annual C input from organic residue i (t ha^{-1}
 207 yr^{-1}), h is its humification or retention coefficient and k is the mineralization rate constant
 208 of the active C pool (yr^{-1}).

209 The bioeconomy co-products are assumed to be composed of two carbon fractions, one
 210 called labile, and another known as stable or recalcitrant. The labile fraction is easily
 211 mineralizable as CO_2 while the recalcitrant fraction is less prone to degradation and is
 212 mineralized at a slower rate than the former one. The size (%) of each fraction and the
 213 time of residence in the soil of the recalcitrant one varies for each co-product in function
 214 of the technology conditions.

215 For the less recalcitrant coproducts (digestate, hydrochar, molasses) the labile fraction
 216 has sizes around 20 – 50%, while the recalcitrant fraction of this group tends to exhibit
 217 MRT values lower than 26 years which are values considered to be close to the MRT of
 218 the active pool. Thus, for this group of products the fraction remaining after one year (h)
 219 is considered to correspond to the recalcitrant fraction defined by the coefficient Cr .
 220 Therefore, Cr is defined as the active retention coefficient (h_a) and is completely allocated
 221 in the active pool C_A where it will be slowly mineralized.

222 The recalcitrant fraction of the highly recalcitrant co-products (pyrochar and gaschar)
 223 constitutes 95% of the coproduct total carbon and exhibit MRTs longer than the 100 years
 224 of simulation conducted here, thus they were treated by way of simplification as inert in
 225 our modeling approach. For this group, the adapted AMG version considered that the
 226 recalcitrant fraction determined by Cr is directly allocated in the C_S pool of the model as

227 the stable retention coefficient (h_s). The labile fraction (5%) is considered to be readily
228 mineralized at the annual time-step.

229 **5. Sensitivity Analyses (SA)**

230 Based on the range of C_c and C_r values reported on (Review), an average result was
231 obtained for the distinct types of feedstocks considered for a given technology. Then the
232 first and third quartiles were selected as a low and a high value, respectively, to be
233 tested in the SA. This approach permitted testing the range of values observed, while
234 not being influenced by the less- likely- to- happen extreme values. This approach
235 resulted in three levels for each parameter.

236 The “main scenarios” for each technology consisted of the combination of the average
237 values of each parameter ($C_{c_{mean}} - C_{r_{mean}}$). The SA constituted new scenarios, which
238 considered the different possible combinations between the two coefficients and the
239 three levels. Combining a mean value with a low or high value would allow identifying
240 the sensitivity of the model to the change in the parameter modified as low or high (i.e.,
241 $C_{c_{mean}}-C_{r_{high}}$ allows to identify the effect of C_r). The combinations between low and
242 high values allowed to identify the combined effect of changing both parameters (i.e.,
243 $C_{c_{low}}-C_{r_{low}}$, $C_{c_{low}}-C_{r_{high}}$, etc.)

244 The way of determining C_r plays a role in the modeled SOC evolution. We considered
245 this source of uncertainty by calculating C_s under two different methods for the
246 pyrolysis scenario.

247 In the **first method**, as explained in the main body, section 2.3.3, we considered that the
248 recalcitrant fraction would be allocated directly in the C_s pool, and we assumed that
249 nothing would be allocated in the active pool C_A .

250 Various modeling assays linked to laboratory incubations and field trials have
251 determined that the recalcitrant fraction would not be inert but would follow a very little
252 decay rate. Therefore, in the **second method**, we determined the amount of C
253 mineralized during the first year based on incubation assays lasting less than 1 year. It
254 was noted that 80% of the labile fraction (5%) would be mineralized in the first couple
255 of months and the other 20% would have a mean life of 10 years (Lehmann and Joseph,
256 2010). In that sense, 4% of the biochar would be directly mineralized in the first year
257 and 1% is allocated in the C_A pool to be slowly mineralized.

258 The C lost in 100 years has been determined by various authors for different crop
259 residues-based biochar (Hammes et al., 2008; Herath et al., 2015; Zimmerman, 2010)
260 using Eq S5 (Lehmann et al., 2015).

$$261 \quad M_t = M_1(1 - e^{-k_1 t}) + M_2(1 - e^{-k_2 t}) \quad (\text{Eq S5})$$

262 where M_t is the Carbon mineralized in mg C g^{-1} biochar at time t , M_1 is the labile
263 mineralizable fraction, M_2 is the recalcitrant C fraction, and k_1 and k_2 are the first-order
264 degradation rate constants for the labile and recalcitrant pools, respectively.

265 Mean values of 26% C lost in 100 years have been obtained in Andrade et al. (2022)
266 from the studies calculating it. This value falls under IPCC (2019) guidelines, which
267 suggest that 80% ($\pm 11\%$) of biochar (pyrolysis, 450-600°C) remains after 100 years.
268 Although evidence suggests that biochar losses in a century could be significantly lower
269 (Zimmerman and Gao, 2013) and the MRT obtained from the ensemble of works in
270 Andrade et al. (2022) at pyrolysis temperatures of 300 – 500°C is 812 years, we opt to
271 be conservative. Therefore, we defined that 75% of pyrochar is inert during the 100
272 years of modeling and is allocated in the C_S pool as the h_s coefficient. After considering

273 the losses in the first year ($1-h_s$), the labile fraction, and the inert fraction (100 years),
 274 the h_a coefficient was calculated to be 0.21 using Eq S6.

275
$$h_{a_pyro} = 1 - (80\%)(C_L) - h_s \quad \text{Eq S6}$$

276 where h_{a_pyro} is the active retention coefficient for the pyrochar scenario alternative
 277 method, C_L is the labile fraction of pyrochar (5%) and h_s is the stable pool
 278 corresponding to the inert fraction of pyrochar for 100 years (75%).

279 As done for the first method, we investigated three levels of h_a and h_s , based on the
 280 mean value and the first and third quartile presented in Andrade et al. (2022). The
 281 combination of “main scenarios” and “SA scenarios” yielded a total of 54 scenarios
 282 explored (Table SI2).

283 Table S1.2. Different combinations of parameters considered for sensitivity. The Cr has
 284 been split between h_a and h_s

Bioeconomy pathways	Recalcitrance (Cr)						(Cc)		
	ha			hs			Low	Mean	High
	Low	Mean	High	Low	Mean	High			
Pyrochar ^a	n/a	n/a	n/a	90	95	99	34	44	54
Pyrochar ^b	36	21	7	60	75	89	34	44	54
Gaschar	n/a	n/a	n/a	90	95	99	14	20	25
Hydrochar	80	83	96	n/a	n/a	n/a	12	31	45
Digestate	58	68	77	n/a	n/a	n/a	29	39	49
Lignocellulosic ethanol molasses	28	45	60	n/a	n/a	n/a	18	24	30

285 Cr : Carbon recalcitrance, h_a : retention coefficient in the active pool, h_s : retention
 286 coefficient in the stable pool, Cc : Carbon conversion

287 ^a First method of introducing Cr for inert fractions in AMG

288 ^b Second method of introducing Cr for inert fractions in AMG

289 n/a under h denotes that the C_A pool was not considered in the model while under C_S

290 denotes that the C_S pool was not considered in the model.

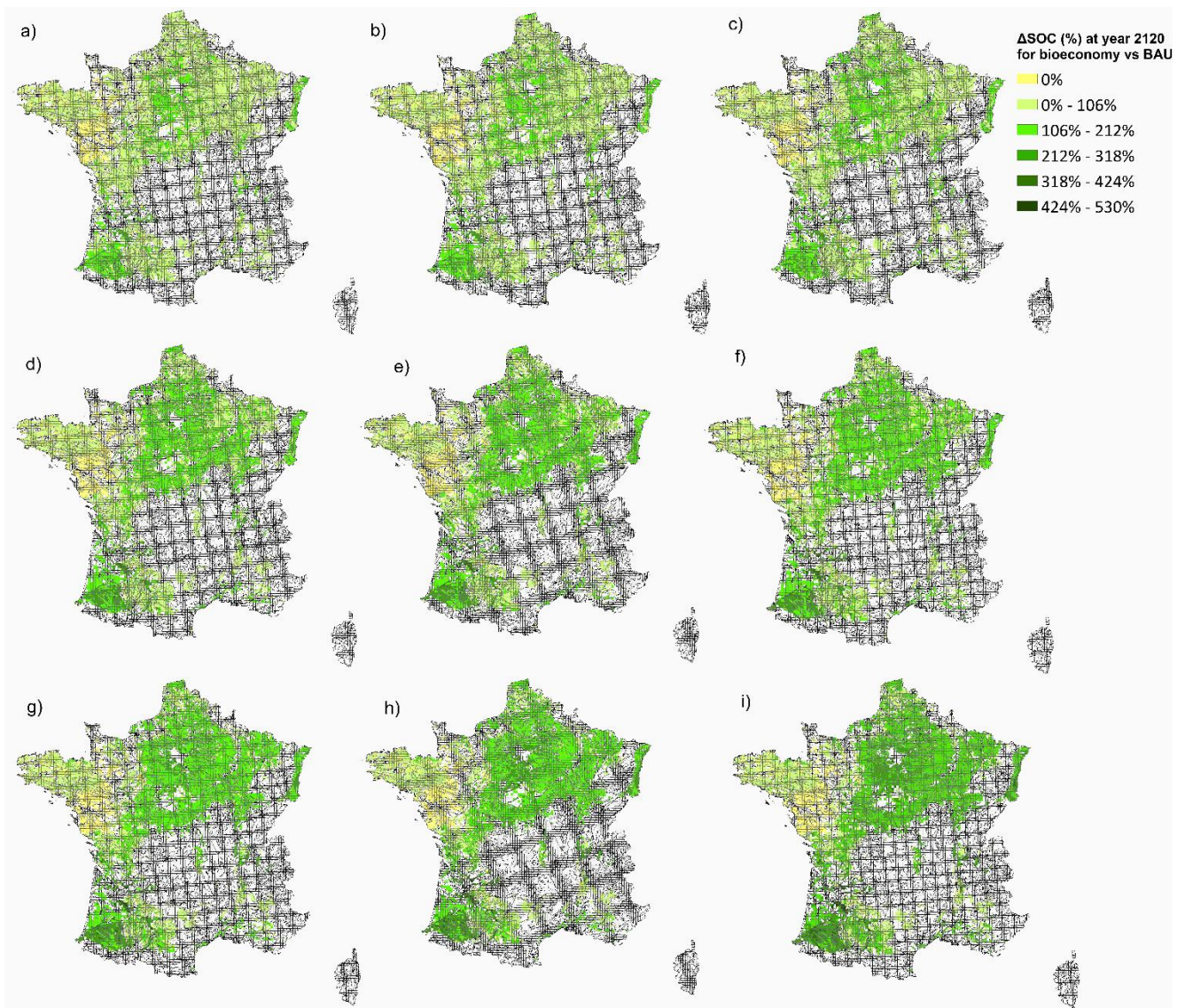
291 A total of 9 extra SA tests were performed to assess the effects of limiting the pyrochar

292 and gaschar application rate and decreasing the exporting rate when SOC losses were

293 observed (AD, HTL, and 2G Ethanol production scenarios).

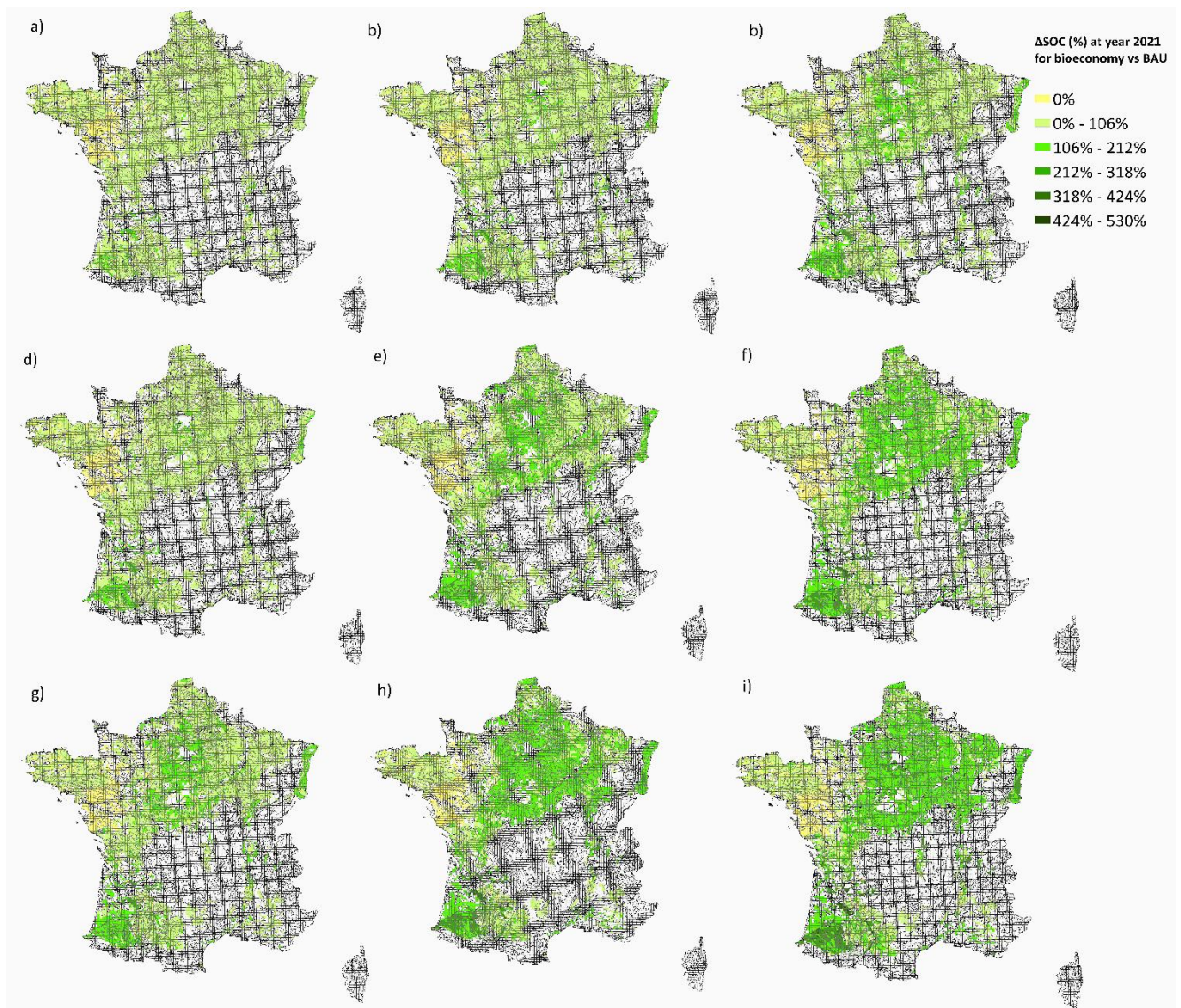
294

295 **SA Result Figures**



296

297 Fig. S4. Sensitivity analyses (SA) for the pyrolysis scenario determined without the
 298 active pool: a) LL: Low Cc – Low Cr, b) LM: Low Cc – Mean Cr, c) LH: Low Cc-
 299 High Cr, d) ML: Mean Cc – Low Cr, e) MM: Mean Cc – Mean Cr (Main scenario), f)
 300 MH: Mean Cc – High Cr, g) HL: High Cc – Low Cr, g) HM: High Cc – Mean Cr, i)
 301 HH: High Cc – High Cr



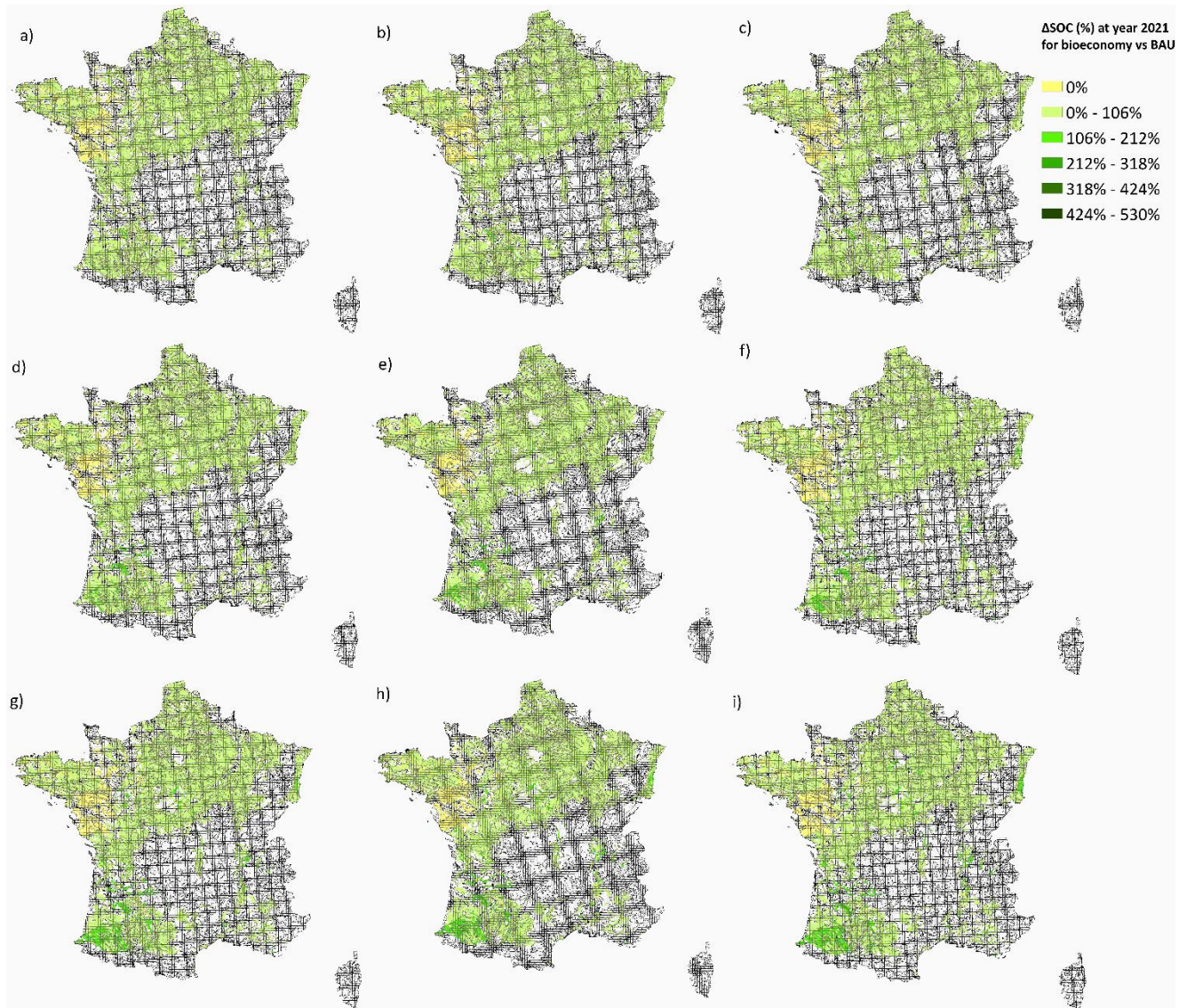
302
 303 Fig. S5. Sensitivity analyses (SA) for the pyrolysis scenario determined with the active
 304 and stable pools: a) LL: Low Cc – Low Cr, b) LM: Low Cc – Mean Cr, c) LH: Low Cc-
 305 High Cr, d) ML: Mean Cc – Low Cr, e) MM: Mean Cc – Mean Cr (Main scenario), f)

306 MH: Mean Cc – High Cr, g) HL: High Cc – Low Cr, g) HM: High Cc – Mean Cr, i)

307 HH: High Cc – High Cr

308

309



310

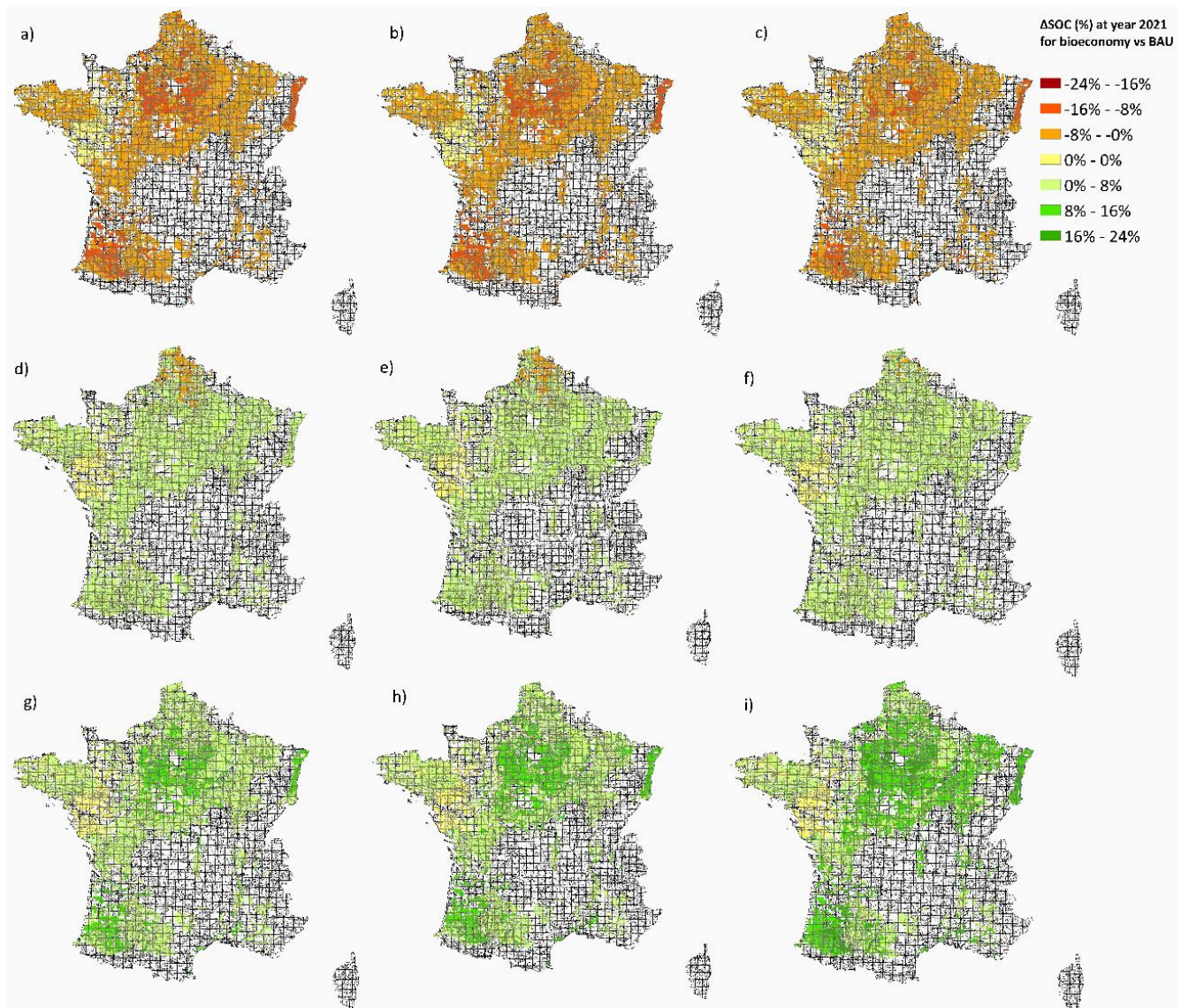
311 Fig. S6. Sensitivity analyses (SA) for the gasification scenario: a) LL: Low Cc – Low

312 Cr, b) LM: Low Cc – Mean Cr, c) LH: Low Cc- High Cr, d) ML: Mean Cc – Low Cr, e)

313 MM: Mean Cc – Mean Cr (Main scenario), f) MH: Mean Cc – High Cr, g) HL: High Cc

314 – Low Cr, g) HM: High Cc – Mean Cr, i) HH: High Cc – High Cr

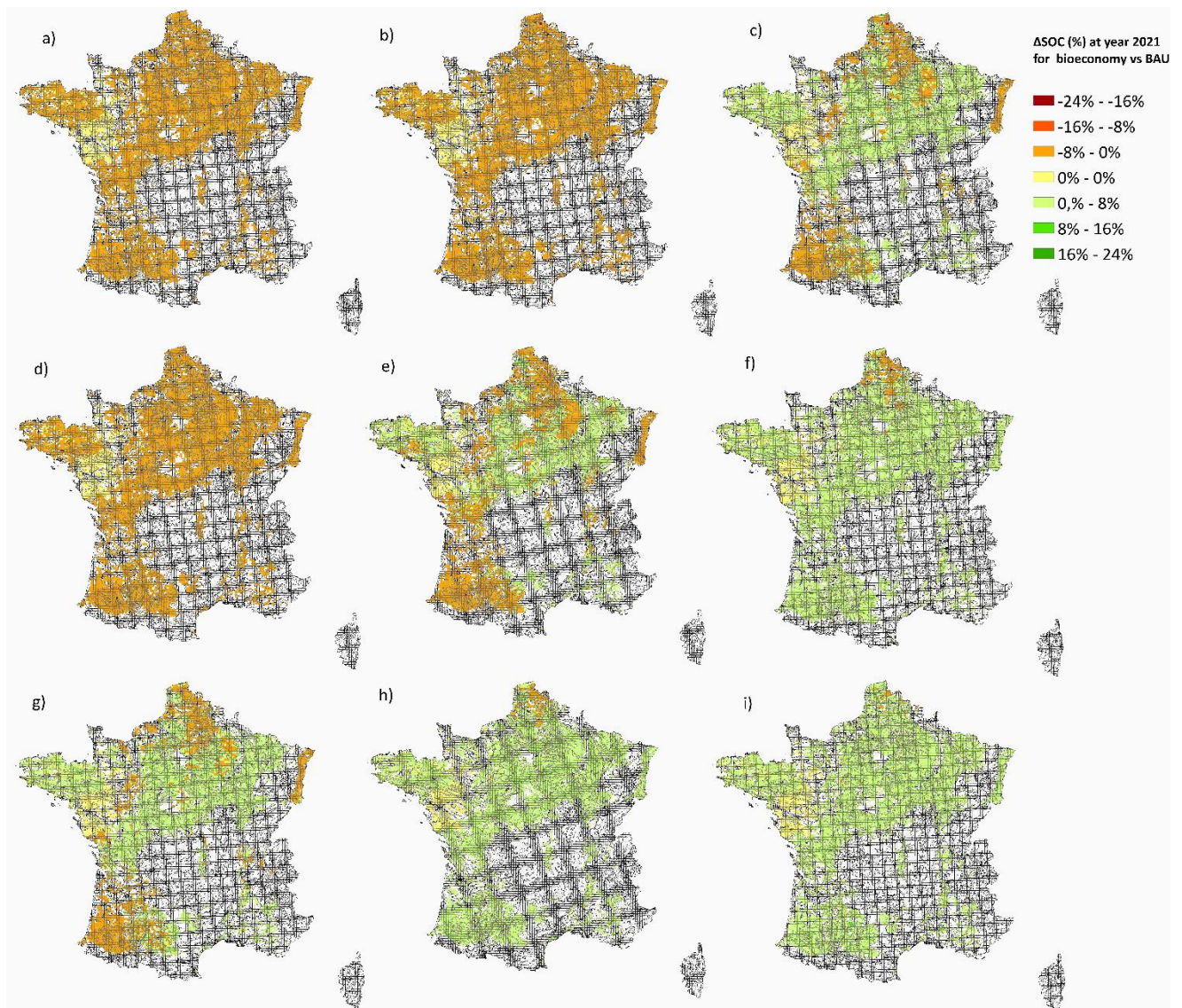
315



316

317 Fig. S7. Sensitivity analyses (SA) for the hydrothermal liquefaction scenario: a) LL:
 318 Low Cc – Low Cr, b) LM: Low Cc – Mean Cr, c) LH: Low Cc- High Cr, d) ML: Mean
 319 Cc – Low Cr, e) MM: Mean Cc – Mean Cr (Main scenario), f) MH: Mean Cc – High
 320 Cr, g) HL: High Cc – Low Cr, g) HM: High Cc – Mean Cr, i) HH: High Cc – High Cr

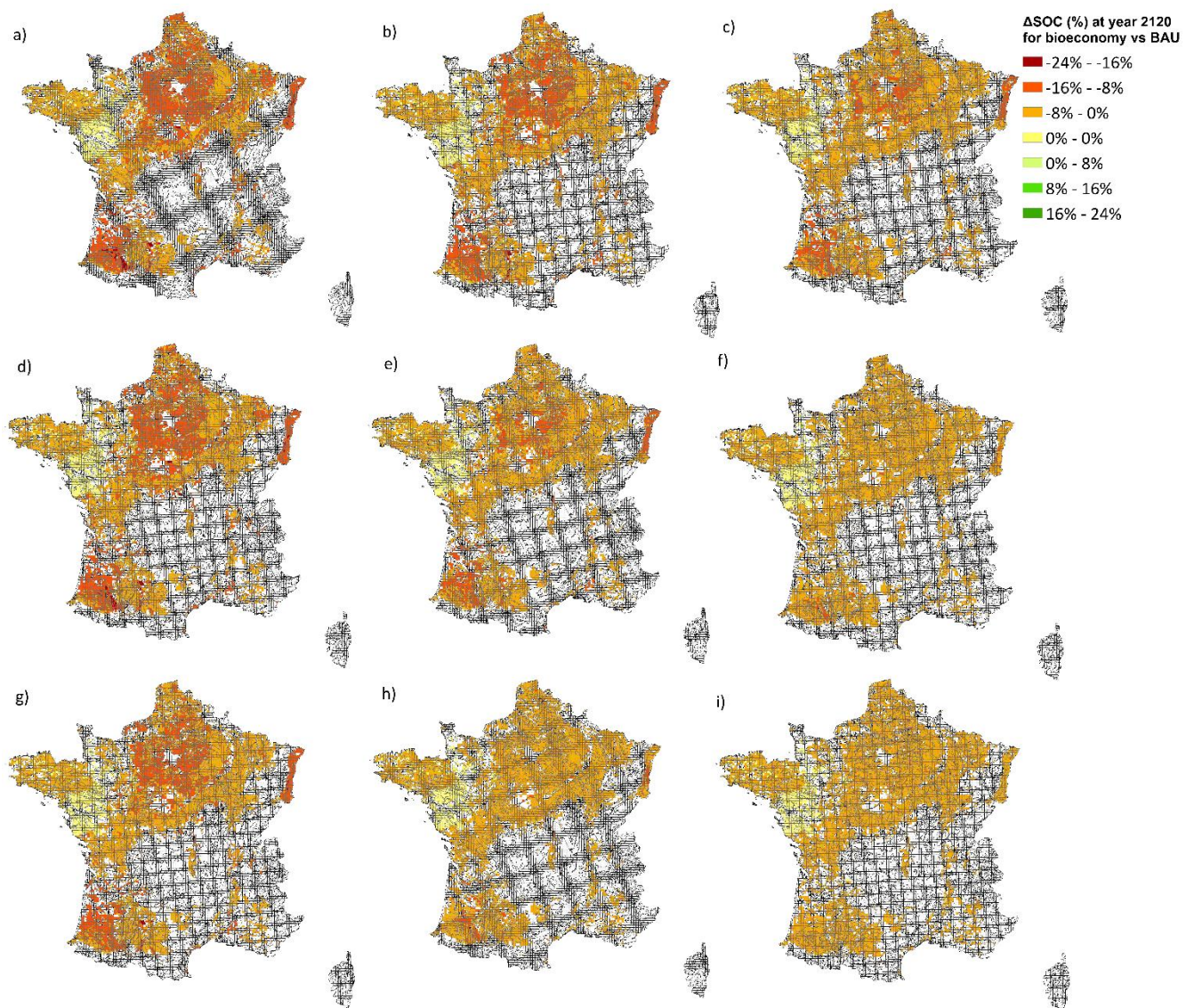
321



322

323 Fig. S8. Sensitivity analyses (SA) for the anaerobic digestion scenario: a) LL: Low Cc –
 324 Low Cr, b) LM: Low Cc – Mean Cr, c) LH: Low Cc- High Cr, d) ML: Mean Cc – Low
 325 Cr, e) MM: Mean Cc – Mean Cr (Main scenario), f) MH: Mean Cc – High Cr, g) HL:
 326 High Cc – Low Cr, g) HM: High Cc – Mean Cr, i) HH: High Cc – High Cr

327



328

329 Fig. S9. Sensitivity analyses (SA) for the lignocellulosic ethanol scenario: a) LL: Low
 330 Cc – Low Cr, b) LM: Low Cc – Mean Cr, c) LH: Low Cc- High Cr, d) ML: Mean Cc –
 331 Low Cr, e) MM: Mean Cc – Mean Cr (Main scenario), f) MH: Mean Cc – High Cr, g)
 332 HL: High Cc – Low Cr, g) HM: High Cc – Mean Cr, i) HH: High Cc – High Cr

333 **References**

- 334 Andrade, C., Albers, A., Zamora-Ledezma, E., Hamelin, L., 2022. A review on the
335 interplay between bioeconomy and soil organic carbon stocks maintenance.
336 PREPRINT (version 1) available at Research Square.
337 <https://doi.org/10.21203/rs.3.rs-1447842/v1>
- 338 Bolinder, M.A., Janzen, H.H., Gregorich, E.G., Angers, D.A., VandenBygaart, A.J.,
339 2007. An approach for estimating net primary productivity and annual carbon
340 inputs to soil for common agricultural crops in Canada. *Agriculture, Ecosystems*
341 *& Environment* 118, 29–42. <https://doi.org/10.1016/j.agee.2006.05.013>
- 342 Clivot, H., Mouny, J.-C., Duparque, A., Dinh, J.-L., Denoroy, P., Houot, S., Vertès, F.,
343 Trochard, R., Bouthier, A., Sagot, S., Mary, B., 2019. Modeling soil organic
344 carbon evolution in long-term arable experiments with AMG model.
345 *Environmental Modelling & Software* 118, 99–113.
346 <https://doi.org/10.1016/j.envsoft.2019.04.004>
- 347 GisSol, 2011. La texture dominante de l’horizon supérieur des sols agricoles par canton
348 [WWW Document].
- 349 Hammes, K., Torn, M.S., Lapenas, A.G., Schmidt, M.W.I., 2008. Centennial black
350 carbon turnover observed in a Russian steppe soil. *Biogeosciences* 5, 1339–
351 1350. <https://doi.org/10.5194/bg-5-1339-2008>
- 352 Herath, H.M.S.K., Camps-Arbestain, M., Hedley, M.J., Kirschbaum, M.U.F., Wang, T.,
353 van Hale, R., 2015. Experimental evidence for sequestering C with biochar by
354 avoidance of CO₂ emissions from original feedstock and protection of native
355 soil organic matter. *GCB Bioenergy* 7, 512–526.
356 <https://doi.org/10.1111/gcbb.12183>

357 IPCC, 2019. 2019 Refinement to the 2006 IPCC Guidelines for National Greenhouse
358 Gas Inventories - Appendix4: Method for Estimating the Change in Mineral Soil
359 Organic Carbon Stocks from Biochar Amendments: Basis for Future
360 Methodological Development. IPCC.

361 Jahirul, M., Rasul, M., Chowdhury, A., Ashwath, N., 2012. Biofuels Production through
362 Biomass Pyrolysis —A Technological Review. *Energies* 5, 4952–5001.
363 <https://doi.org/10.3390/en5124952>

364 Joly, D., Brossard, T., Cardot, H., Cavailles, J., Hilal, M., Wavresky, P., 2010. Les
365 types de climats en France, une construction spatiale. *Cybergeo : European*
366 *Journal of Geography* [En ligne], Cartographie, Imagerie, SIG.
367 <https://doi.org/10.4000/cybergeo.23155>

368 Launay, C., Constantin, J., Chlebowski, F., Houot, S., Graux, A., Klumpp, K., Martin,
369 R., Mary, B., Pellerin, S., Therond, O., 2021. Estimating the carbon storage
370 potential and greenhouse gas emissions of French arable cropland using high-
371 resolution modeling. *Glob. Change Biol.* 27, 1645–1661.
372 <https://doi.org/10.1111/gcb.15512>

373 Lehmann, J., Abiven, S., Kleber, M., Pan, G., Singh, B.P., Sohi, S.P., Zimmerman,
374 A.R., 2015. Persistence of biochar in soil, in: *Biochar for Environmental*
375 *Management*. p. 48.

376 Lehmann, J., Joseph, S. (Eds.), 2010. *Biochar for environmental management: science*
377 *and technology*, Reprint. ed. Earthscan, London.

378 Malyan, S.K., Kumar, S.S., Fagodiya, R.K., Ghosh, P., Kumar, A., Singh, R., Singh, L.,
379 2021. Biochar for environmental sustainability in the energy-water-
380 agroecosystem nexus. *Renewable and Sustainable Energy Reviews* 149, 111379.
381 <https://doi.org/10.1016/j.rser.2021.111379>

382 Molino, A., Chianese, S., Musmarra, D., 2016. Biomass gasification technology: The
383 state of the art overview. *Journal of Energy Chemistry* 25, 10–25.
384 <https://doi.org/10.1016/j.jechem.2015.11.005>

385 Seehar, T.H., Toor, S.S., Sharma, K., Nielsen, A.H., Pedersen, T.H., Rosendahl, L.A.,
386 2021. Influence of process conditions on hydrothermal liquefaction of
387 eucalyptus biomass for biocrude production and investigation of the inorganics
388 distribution. *Sustainable Energy Fuels* 5, 1477–1487.
389 <https://doi.org/10.1039/D0SE01634A>

390 Swain, M.R., Singh, A., Sharma, A.K., Tuli, D.K., 2019. Chapter 11 - Bioethanol
391 Production From Rice- and Wheat Straw: An Overview, in: *Bioethanol*
392 *Production from Food Crops. Sustainable Sources, Interventions, and*
393 *Challenges*. Academic Press, p. 19.

394 Tonini, D., Hamelin, L., Astrup, T.F., 2016. Environmental implications of the use of
395 agro-industrial residues for biorefineries: application of a deterministic model
396 for indirect land-use changes. *GCB Bioenergy* 8, 690–706.
397 <https://doi.org/10.1111/gcbb.12290>

398 University of Zagreb, Faculty of Food Technology and Biotechnology, Pierottijeva 6,
399 10000 Zagreb, Croatia, Bušić, A., Marđetko, N., University of Zagreb, Faculty
400 of Food Technology and Biotechnology, Pierottijeva 6, 10000 Zagreb, Croatia,
401 Kundas, S., Belarussian National Technical University, Power Plant
402 Construction and Engineering Services Faculty, Nezavisimosti Ave. 150,
403 220013 Minsk, Belarus, Morzak, G., Belarussian National Technical University,
404 Mining Engineering and Engineering Ecology Faculty, Nezavisimosti Ave. 65,
405 220013 Minsk, Belarus, Belskaya, H., Belarussian National Technical
406 University, Mining Engineering and Engineering Ecology Faculty,

407 Nezavisimosti Ave. 65, 220013 Minsk, Belarus, Ivančić Šantek, M., University
408 of Zagreb, Faculty of Food Technology and Biotechnology, Pierottijeva 6,
409 10000 Zagreb, Croatia, Komes, D., University of Zagreb, Faculty of Food
410 Technology and Biotechnology, Pierottijeva 6, 10000 Zagreb, Croatia, Novak,
411 S., University of Zagreb, Faculty of Food Technology and Biotechnology,
412 Pierottijeva 6, 10000 Zagreb, Croatia, Šantek, B., University of Zagreb, Faculty
413 of Food Technology and Biotechnology, Pierottijeva 6, 10000 Zagreb, Croatia,
414 2018. Bioethanol Production from Renewable Raw Materials and its Separation
415 and Purification: a Review. *Food Technol. Biotechnol.* 56.
416 <https://doi.org/10.17113/ftb.56.03.18.5546>

417 Zimmerman, A., Gao, B., 2013. The Stability of Biochar in the Environment, in:
418 Ladygina, N., Rineau, F. (Eds.), *Biochar and Soil Biota*. CRC Press, pp. 1–40.
419 <https://doi.org/10.1201/b14585-2>

420 Zimmerman, A.R., 2010. Abiotic and Microbial Oxidation of Laboratory-Produced
421 Black Carbon (Biochar). *Environ. Sci. Technol.* 44, 1295–1301.
422 <https://doi.org/10.1021/es903140c>

423